Laboratory tests for the evaluation of the degradation of a photovoltaic plant of 2.85 MWp with different classes of PV modules

J.A. Clavijo-Blanco [a,*], G. Álvarez-Tey [a], N. Saborido-Barba [a], J.L. Barberá-González [a], C. García-López [a] and R. Jiménez-Castañeda [a]

[a] *Department of Electric Engineering, Superior College of Engineering, University of Cádiz Campus Universitario de Puerto Real, 11519 Puerto Real (Cádiz), Spain.*

Abstract

This paper studies and analyzes the results of performing several laboratory tests of a sample from a PV-plant with 2.85 MW of nominal power that has been in operation for 11 years and whose PV-modules are from different manufacturer and classes. The main purpose is to develop a proper quality inspection that allows knowing the degradation in a PV-plant with these special characteristics. The total sample has been taken in proportion to the size of each class through a proportionate allocation stratified sampling strategy. The tests performed on each sample were detailed visual inspection, power rating, electroluminescence (EL), and electrical insulation. The PV modules tested have been analyzed and evaluated according to an acceptance/rejection criteria established by the laboratory which has been based on International Electrotechnical Commission standards, bibliographic contributions and the warranty conditions of PV-modules. Considering the age of the plant and the criteria established in the power rating, the 80.01% of the sample modules were in good conditions, the 10.27% degraded and the 9.72% rejected. The results also show that the total annual average degradation rate of the PV-plant after 11 years of operation is 0.94%/year.

Keywords: Electroluminescence (EL), I-V curves, Visual inspection, Quality inspection, Annual degradation rate

1. Introduction

The reduction of carbon and greenhouse gas emissions to limit climate change impact are global issues which have led to a change in electric energy markets worldwide. Among all renewables technologies, large-scale solar photovoltaic (PV) power plants have been broadly installed around the world in recent years. According to Solar Power Europe in [1], the total world installed PV power capacity reached 633.7 GW by the end of 2019, resulting in a 23% year-on-year grown compared to 2018 (509.3 GW). Furthermore, the future projection based on IRENA

**Corresponding author.*
Email addresses: joseantonio.clavijo@uca.es, german.alvarez@uca.es, nieves.saborido@uca.es, joseluis.barberagonzalez@alum.uca.es, carmen.garcia@uca.es and rafael.castaneda@uca.es.
"This work was supported in part by INOMA Renovables S.L.".

analysis, which is reported in [2], cumulative solar PV capacity is expected to grow sixfold by 2030, with a compound annual growth rate of nearly 9% up to 2050.

For current and future large-scale PV plants, stakeholders are interested in improving its reliability optimizing operational and maintenance (O&M) cost to secure the invested capital and profit [3]. In this context, to secure the profitability and to provide effective follow-up along the lifetime of a PV plant, quality inspections, which could be scheduled in preventive maintenance plans, gain a particular interest [4].

The study of the degradation, defects and failures in PV plant has taken certain significance through times due to the importance of getting an accurate prediction of the performance of these systems [5]. Environmental conditions may have an important influence on the degradation rate. Therefore, the degradation rate studies from diverse geographical locations are of great interest [6], since ageing, performance and degradation are a phenomenon that affects the power system output and consequently financial figures of merit [7]. In ref. [7] has been also observed that higher degradation rates are reported when harsher climatic regions are studied. The value reported in [8] resulted greater than the 0.8%/year in only 3 years of outdoor exposure in Morocco.

To determine the annual degradation rates of PV modules, three parameters are usually taken into account: energy efficiency, output performance ratio and electrical power [9]. These parameters could be studied through the performance of different tests that are usually based on visual inspection, infrared thermography [10], [11], [12] and electrical monitorization, which can sense the overall behaviour of the PV plant [13], [14] or performing diagnoses at the panel level [15]. However, each monitorization technique used for the diagnosis, the measuring of the equipment and the quality of the data may lead to different results [16]. An example could be observed in [17], where some authors have measured the output power of a PV plant to study the presence of dust on the panel surface. It has been also applied alternative methods which have been performed in small plants to measure both the IV curves of each module [18] and the electrical monitorization in different technologies [19].

PV panel laboratory tests have also been carried out to study degradation, power losses and efficiency. In this case, test mainly used for failure detections, which are defined in [20], are visual inspection [21], IR thermography [22], [23], indoor and outdoor power measurements using I-V curve tracers [24], [25] and electroluminescence (EL) [9]. To get a different evaluation of the possible defects found in a PV-plant, as may be the power induced degradation (PID), results of PV modules tested in laboratories can be contrasted with those tested outside, which may lead to improve the reliability of the outcome [8]. Furthermore, several tests may be performed over several sample modules of a PV plant as has been done in [26], where 48 sample modules have been submitted to visual inspection, electroluminescence and I-V curves measurement resulting in several defects founded and a global average degradation of 9.5% during 15 years of outdoor exposure.

The paper presents a quality inspection methodology through laboratory test with an acceptance and rejection criteria established by the laboratory itself that get practical results about the degradation of a PV-plant operating with different classes of PV modules. Results allowed to

estimate the annual average degradation rate of the PV-plant according to each manufacturer. Although they all were operating in the same emplacement, the results obtained were different to one from another due to the quality of the PV modules presented by each manufacturer.

This article is structured as follows: the second section shows the experimental data of the PV plant, the third section shows the methodology established by the laboratory, the fourth section shows the acceptance and rejection criteria, in the fifth section is where the results are shown and discussed, the sixth section presents the annual degradation rate of the PV plant estimated by a Gauss-Newton algorithm, and finally, in the seventh section, the conclusions are bulleted.

2. Experimental data

The PV plant has a rated power of 2.85 MW and was commissioned in 2008. It is located in the south of Spain and consists of a total of 29 inverters, of which 28 have a rated power of 100 kW and 1 has a rated power of 50 kW. The PV plant is nowadays composed of a total of 18 classes of different PV modules of polycrystalline technology from 5 different manufacturers. Table I shows the electrical features of the PV-modules which were operating in the PV power plant.

Table I: PV-modules electrical features.

PV module	Brand	PV module class (Wp)	Vmp (V)	Imp (A)	Voc (V)	Isc (A)	Maximum Power (MPP) (W)	MPP Tolerance rating (%)	Number of samples
ET SOLAR	1	270	36.40	7.42	43.63	8.10	270.00	±3	98
TYNSOLAR 220P6	2	195	24.53	7.96	29.52	8.46	195.00	±5	3
		200	24.96	8.03	29.76	8.52	200.00	±5	10
		205	29.58	6.93	35.94	7.47	209.90	±5	33
		210	29.64	7.09	35.94	7.60	214.90	±5	30
		215	29.94	7.18	36.00	7.83	219.90	±5	30
		220	30.12	7.30	36.06	7.95	224.90	±5	72
		225	30.36	7.41	36.42	8.10	229.90	±5	49
		230	30.48	7.55	36.60	8.17	234.90	±5	8
CANADIAN SOLAR	3	210	46.60	4.51	57.90	4.94	210.00	±5	5
		220	46.90	4.69	58.40	5.10	220.00	±5	7
		230	47.50	4.84	58.80	5.25	230.00	±5	10
		235	29.80	7.90	36.90	8.46	235.00	±5	3
		240	48.10	4.99	59.30	5.40	240.00	±5	2
ATERSA	4	210	28.99	7.38	36.02	8.03	210.00	±5	-
		215	-	-	-	-	-	±5	-
		220	29.47	7.59	36.14	8.38	220.00	±5	-
SOLARDAY PX72	5	260	34.10	7.60	44.40	8.17	260.00	±5	-

A PV modules inventory database, which has been provided by the electric company responsible for the operation of the plant, has been studied. According to the database provided, PV modules brands 1, 2 and 3 were initially installed in the solar plant, which currently represent the 27.12%, 64.50%, and 6.67% of the total PV modules installed. PV modules brand 4 and brand 5, which represent 1.42% and 0.28% respectively, were used to replace defectives PV modules of brands 1 and 2. PV modules were replaced directly by PV modules according to their rated power in STC. No string reconfiguration was done, no photocurrent testing or annual degradation was taken into account. This procedure may aggravate the degradation of the PV-arrays due to electrical mismatches by the use of different classes or manufacturer [27].

In this work, only brands 1, 2 and 3, which represent the 98.29%, has been taken into consideration to the study of the degradation of the PV plant during its years of operation. A sampling method has been used to select PV panels, which has been described in the methodology. A total of 360 sample modules has been analyzed.

Since sample modules had to be disconnected by an experienced technician, each sample was previously labelled during an on-site visit. The electrical coding available on the layout did not allow easy identification of the modules in the plant, so, a new codification focused on the physical location instead of an electrical code was established to label all sample modules [28].

To minimize the impact of disconnecting and connecting PV modules in the plant, PV modules were disconnected and sent to our labs in 3 different packs. Until a pack of PV did not return to the PV plant the second was not sent. The transport and reloading of PV modules cause cell cracks [21], so, to minimize it, they were conveniently packed up.

The on-site PV visit has been performed in May 2019. Apart from the labelled of the sample modules, a quality inspection was also performed. It consisted of three different tests: visual inspection, IR thermography and electrical monitoring. Tests have been based on the standard and technical specification published by the International Electrotechnical Commission (IEC) 61215-1-1:2016 [29], 62446-3:2015 [30] and 61724-1:2017 [31] respectively. Results were published in [28], and according to the IR thermography inspection performed, less than 1% of PV modules installed in the power plant shown thermal defect, while, according to the electrical monitoring, it was noticeable that those inverters whose PV arrays contained different classes of PV modules injected slightly less energy.

All sample modules were subjected to four tests; detailed visual inspection, I-V curve tracing, electroluminescence and electrical isolation. Before carrying out the tests, all of them were cleaning with neutral detergent and distilled water to remove surface dirt deposits from the glass. The methodology employed in each test is described below.

3. Methodology

3.1. Sampling method

A stratified random sampling with proportional allocation has been applied to obtain the size of the sample getting results with a 95% of confidence level. The population has been divided into several homogenous groups. The size of each stratum has been taken randomly and in proportion to the size of each group. Thus, the size of the sample represents the total number of PV modules tested while each stratum represents each PV module brand found in the PV plant. The sampling procedures applied in this paper has been based on the standard published by the International Standard Organization 2859-1:1999 [32].

The population considered in the probability sampling method proposed was the 98.29 % of the PV modules installed in the PV plant. This percentage included PV modules from brands 1, 2 and 3 which have been operational since the commissioning of the PV plant. PV modules installed to

replace defective PV modules has not been included, which represent the 1.71% of the PV plant. As a result, a total of 360 sample modules were tested. The number of sample modules needed for each brand is shown in Table I.

Once the sample modules were chosen and labelled in the PV-plant, they were disconnected and carried to our labs, where were subjected to different tests.

3.2. Visual Inspection

The detailed visual inspection has been performed on all the sample modules to find observables defects. It has been based on the standard IEC 61215-1-1:2016 [29], whose images have been also studied according to [21]. Visual inspection was performed exteriorly and always with an illuminance greater than 1000 lux. A picture of each PV module was taken while a checklist was used to write down all visible failures detected.

3.3. Electrical inspection: power rating

To be able to evaluate the total power loss and the yearly degradation of the sample modules, the current-voltage (I-V) curve of each one were measured with the I-V tracer PVPM 6020C under field conditions. It was measured based on the proceeding published by IEC 61215-2:2016 [33], where, to get good results, the minimum required irradiance level for the measure was set to 700 W/m^2 over PV modules surface. Measurements were conducted between 12:00 and 2 p.m. local time.

Once taken, I-V curves were then extrapolated to standard test conditions (STC) based on procedure 1 described in the IEC 60891:2009 [34]. The translation parameters α and β were supplied by the PV modules datasheets while the incident irradiance and the operating cell temperature was measured using a calibrated PV cell included in the I-V tracer.

The PV panel total degradation (R_T) was obtained using ΔP_{max} as shown below:

$$R_T(\%) = \frac{\Delta P_{max}}{P_{max,0}} = \frac{P_{max,0} - P_{max,STC,i}}{P_{max,0}} \quad (1)$$

Where,

- $P_{max,0}$; PV panel maximum peak power according to the datasheet in STC conditions.
- $P_{max,STC,i}$; PV panel maximum peak power tested and extrapolated to STC in the year i.

3.4. Electroluminescence

To analyze cell cracks in PV modules, all the sample modules were subjected to electroluminescence (EL). During the EL test, several images with high spatial resolution were taken. EL images provided with high spatial resolution allow detecting even the most insignificant PV cell cracks. This test was performed in an indoor laboratory by the EL CAM XENICS SWIR camera Bobcat 320. EL images were taken based on the technical specification published by the

IEC 60904-13:2018 [35], where, each sample has been polarized in a dark environment through the injection of direct current (DC). Polarized PV cells emit radiation that is captured by an electroluminescence camera [21].

The control of the operation of the EL camera was made by a specific software which was included in the CAM equipment. This software allowed selecting the optimal filter, as well as the modification of settings, among other functions. A filter is used to reduce the interference light from other sources.

For each sample, it has been obtained three EL images. The first EL image was taken without polarizing the sample. The second EL image was taken polarizing the sample with a current similar to 10% of the PV module short-circuit current in STC. And finally, the third EL image was obtained polarizing the sample with a current similar to 100% of the PV module short-circuit current in STC. This procedure allows getting the size of the cracks in different operating condition. Fig. 1 shows an example of different PV modules subjected to both currents. It can be seen that results can vary significantly from one to another, being the size of the cracks more marked when the sample is polarized with a current similar to 100% Isc.

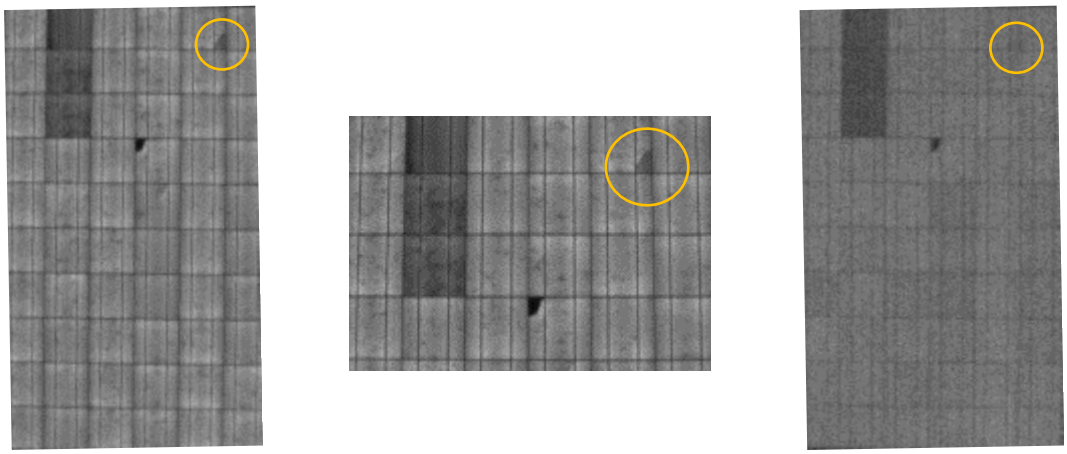

a) b) c)

Fig. 1. Electroluminescence (EL). a) 100% Isc, b) 100% Isc (Zoom), c) 10% Isc

3.5. Electrical insulation.

To evaluate the electrical insulation of the sample modules, the insulation resistance has been measured through the FLUKE 1550B. The test has been made based on the standard IEC 61215-2:2016 [33], which mainly consist of two stages:

- Stage 1: The PV module is subjected to a ramp voltage of 500 V/s up to 3000 V, maintaining such voltage for 1 minute.
- Stage 2: The PV module is subjected to a ramp voltage of 500 V/s up to 1000 V, maintaining such voltage for 2 minutes.

198 The final result is taken from stage 2.

199

200 **4. Acceptance/rejection criteria**

201 The PV modules tested have been analyzed and evaluated according to an acceptance/rejection
202 criteria established by the laboratory which has been based on the level of degradation presented
203 by each module. Considering the age of the plant, the location and technology used, the criteria
204 establish fit those modules with less than 15% of degradation, degraded with a degradation
205 between 15% and 20% and unfit those modules with a degradation greater than 20%.

206 The remaining tests that were carried out intend to expand information on the origin and nature
207 of the defects/failures, considering reference values to evaluate them.

208 *4.1. Visual Inspection*

209 According to [21], defects may be the reason for some PV modules no performing as well as
210 possible while module failures are no-reversed defects that produce power loss or safety issues.
211 So, as rejection criteria, it has been considered as non-acceptable those failures who produce a
212 considerable power loss or safety issues. Although this has been discussed in results and
213 summarized in Table II, those sample modules with the front glass broken or affected by burned
214 marks in PV cells have been rejected. It is because the sample modules which suffer from these
215 failures shown greater power loss, safety issues or both at the same time. For example, as it has
216 been also reported in ref. [36], PV modules with broken front glass counted as a severe/strong
217 damage which has a direct impact on the yield of the PV-plant apart from being a hazard safety
218 issue.

219 *4.2. Electrical inspection: power rating*

220 According to [6], where nearly 2000 degradation rates have been assembled, the majority of the
221 data reported a degradation rate of <1%/year, whose mean and median values are 0.8%/year and
222 0.5%/year respectively. However, the degradation also needs to be interpreted in the context of
223 the useful life of a solar panel and the manufacturer warranty, being both commonly established
224 in 25 years in [6] and [37]. During its useful life, PV modules are expected to not get a power loss
225 greater than the 20% [7]. So, with exception of early exposure and end-of-life stages, if the module
226 degradation is considered linear [7], [38], the average annual degradation rate of the module´s
227 maximum power according to the manufacturer warranty ($WADR_{Pmax}$) is determined as:

228 $$WADR_{Pmax} = \frac{WP_{loss}}{w_y} \qquad (2)$$

229 Where WP_{loss} is the power loss in % and w_y the years of modules warranty. The manufacturers
230 guarantee a maximum PV module power loss during a certain time, being usually the 20% of the

rated power during 20-25 years [20]. Considering the age of the PV plant when tests were performed, the $WADR_{Pmax}$=1%.

Once I-V tracer test was performed and its results extrapolated to STC, the R_T was obtained in each sample. The acceptance/rejection criteria were established by the laboratory according to the exposure time of the modules, the location of the PV plant, the warranty condition, the manufacturer features, the references cited and its own experience in the field. Thus, the results were then clustered in three levels of degradation:

- **Fit modules** for those that presented a power degradation lower than 15%. This level of degradation has been established taking into consideration the $WADR_{Pmax}$, the age of the PV plant when tests were performed and the most unfavorable manufacturer tolerance shown in Table 1.
- **Degraded modules** for those that presented a degradation between 15% and 20%. This level of degradation tries to cluster those sample modules that had a considerable degradation but it did not get over the threshold of 20% of power loss.
- **Unfit modules** for those that presented a degradation greater than 20%.

Finally, as acceptance/rejection criteria, those sample modules with a power loss greater than 20% were labelled as non-acceptable since it fell below the minimum acceptable level established by the laboratory. So, those sample modules with a power loss lower than 20% were labelled as acceptable, evaluating as degraded those whose power loss were closer to the warranty threshold.

Once all the sample modules were evaluated according to the acceptance/rejection criteria established, there was a need for more deep analysis and try to obtain the annual degradation of the PV panels installed in the PV power plant. Therefore, the annual degradation of each sample has been obtained.

In this paper, the module degradation has been assumed as linear during the exposure time. Ref. [6] reported that the degradation appeared to be linear for 22 years of exposure, however, it appeared to increase after 30 years of exposure. A linear degradation through time has been already considered in similar studies, such as [7] and [38]. So, the annual degradation rate of each sample (ADR_{Pmax}) was determined as:

$$ADR_{Pmax} = \frac{WP_{loss}}{y} \qquad (3)$$

Where WP_{loss} is the power loss of the PV modules in the maximum power point in STC and y the exposure time.

4.3. Electroluminescence

To evaluate the EL images, three types of cracks were established based on the technical specification IEC 60904-13[35], where three cell crack types (A, B and C) are distinguished according to the power loss causes on the sample. A-cracks do not cause significant cell power loss, B-cracks do not imply a significant power loss and C-cracks delimit electrically disconnected

areas from the PV module which can lead to a significant power loss. Each cell crack type is shown in Fig. 2.

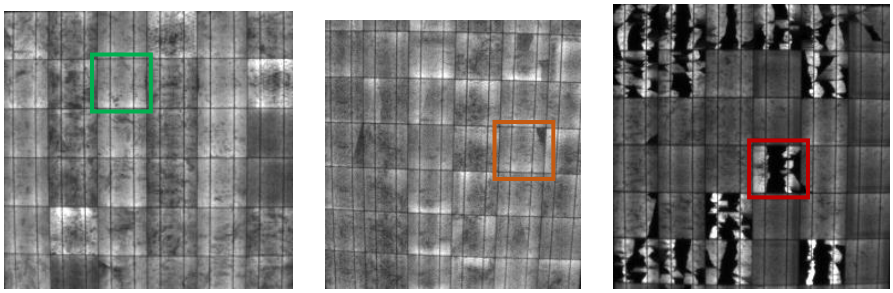

a) b) c)

Fig. 2. Types of cracks in several sample modules. a) A-cracks, b) B-cracks, c) C-cracks

Depending on the pattern of the cracks observed in an EL image, the PV cells can be affected by inactive areas, which will no longer contribute to the power output of the PV module. In this context and according to [39], when an inactive part of a PV cell is greater than 8% of the total cell area, it results in a significant power loss which increases linearly with the inactive cell area. Since cell cracks class A and B are not involved with a considerable power loss, as acceptance and rejection criteria, those sample modules whose inactive area was greater than 8% due to cracks class C were considered as non-acceptable.

4.4. Electrical insulation

The acceptance/rejection criteria of this test have been based on IEC 61215-2:2016 [33], where those sample modules with an area greater than 0.1 m^2, the product of the insulation resistance measured in stage 2 of the test procedure and the total area of the PV module must not be lower than 40 $M\Omega/m^2$.

5. Results

The results obtained through the different test done in labs are developed in this section. The results are shown in an orderly manner according to the followed methodology; detailed visual inspection, power rating, electroluminescence and electrical insulation.

5.1 Detailed visual inspection

Several defects have been found in the detailed visual inspection. Fig. 3 shows the different defects found for each PV module class, where it can be seen that the browning is the most recurrent defect, with a 29.95% of the total, followed by yellowing, back sheet scratches and anti-reflective layer, with the 21.39%, 12.57% and 12.03% respectively.

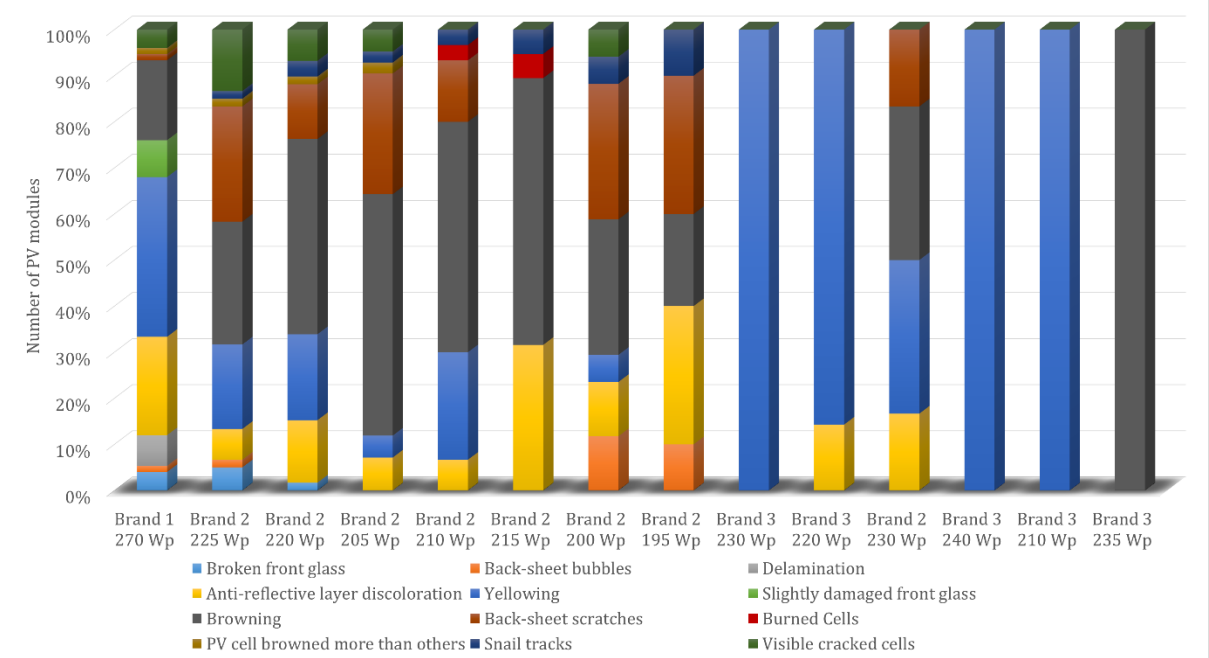

Fig. 3. Detailed visual inspection results by PV module class

Once the defects were quantified, they were clustered in two groups according to the power loss associated. The first group contain defects which do not have a strong relationship with the power loss and do not suppose any safety issues. In this group, there is not any way to relate the visual defect with a severe power loss, since it can vary from little to great value. The second group contain failures which had a strong relationship with a considerable power loss or safety issues and may be detected by a simple glance.

In Fig. 4 several graphics are presented where each one represents the defects found. For each graphic, it is shown the relationship between the presence of the defect and the power loss in each sample, where it can be seen that the majority of the defects do not have a strong relationship between its occurrence and its power loss associated. For example, in Fig. 4. d) there exist lots of sample modules which suffer from yellowing and had a different power loss associated, which can vary from 0% to 100%. The same occurs with the rest of defects except for broken front glass and burn marks in PV cells, which graph are shown in Fig.4. a) and Fig.4. I), and had always a considerable power loss associated. Additionally, all the sample modules affected by these two defects may also cause important safety problems according to [21]. The analysis of each visual defect found is summarized in Table II. For this reason, broken front glass and burn marks in PV cells were categorized as a failure and considered as non-acceptable under the visual inspection test.

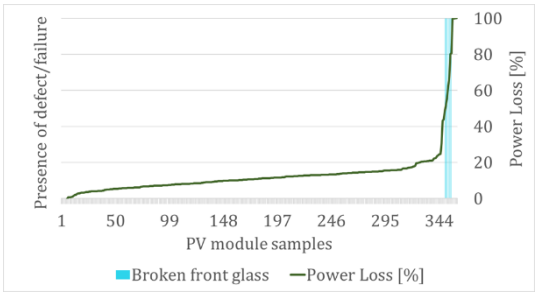

a) Broken front glass

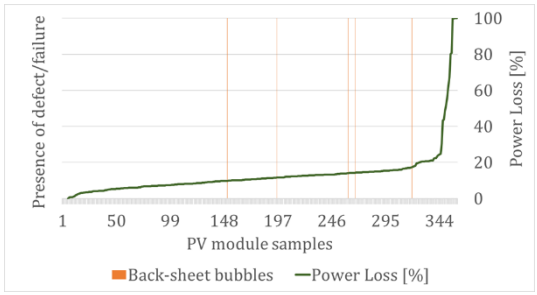

b) Back-sheet bubbles

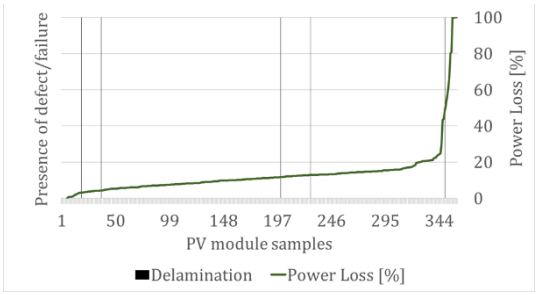

c) Delamination

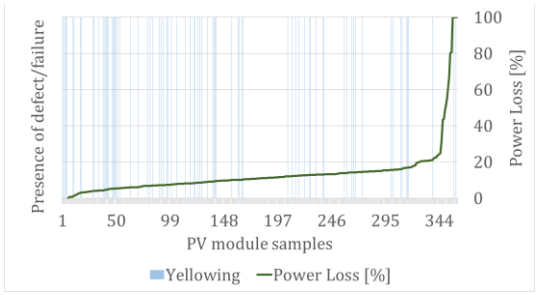

d) Yellowing

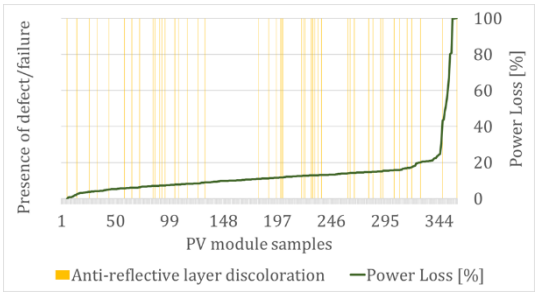

e) Anti-reflective layer discoloration

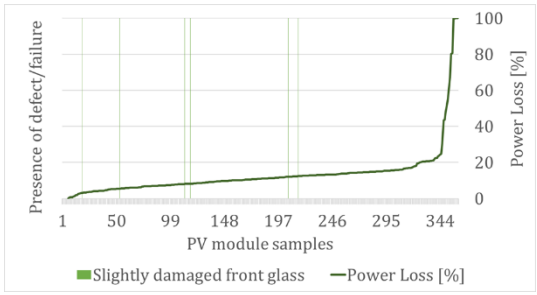

f) Slightly damage front glass

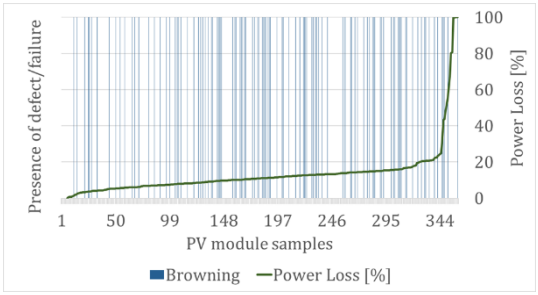

g) Browning

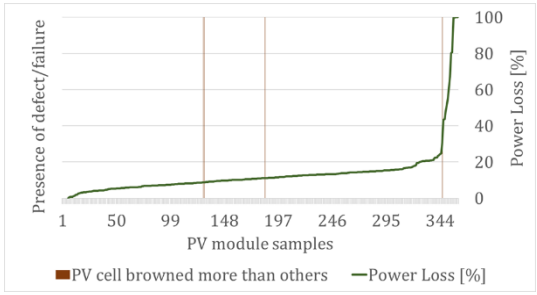

h) PV cell browned more than others

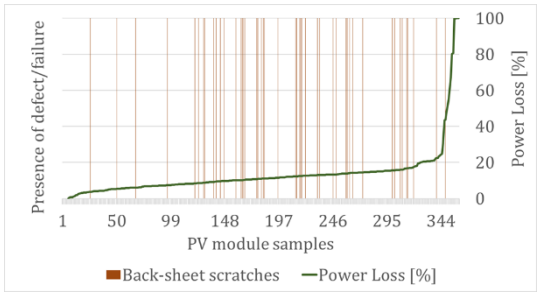

i) Back-sheet scratches

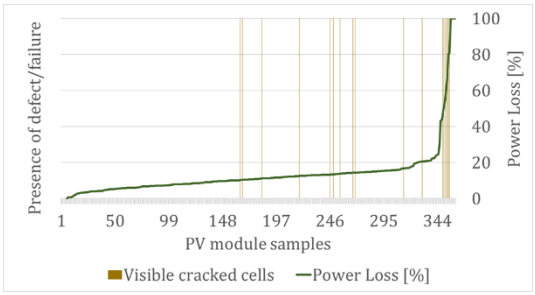

j) Visible cracked cells

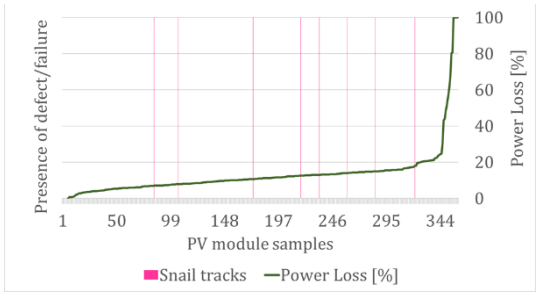

k) Snail tracks

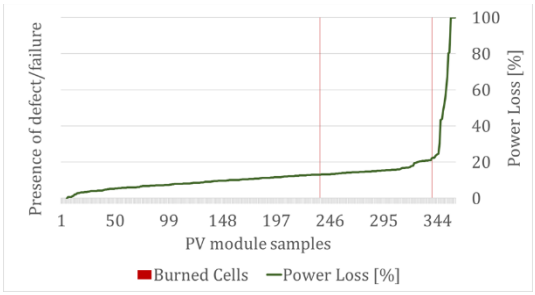

l) Burn marks

Fig. 4. Relationship between visual defects and power losses in the sample modules.

It has been assumed that the impact of each defect on the power loss is independent. However, it may be possible that some defect combined had a stronger impact on the power loss. Fig. 5 shows defectives PV modules and their associated power loss. In this figure, it can be seen that the maximum number of defects found in a single PV module is 4.

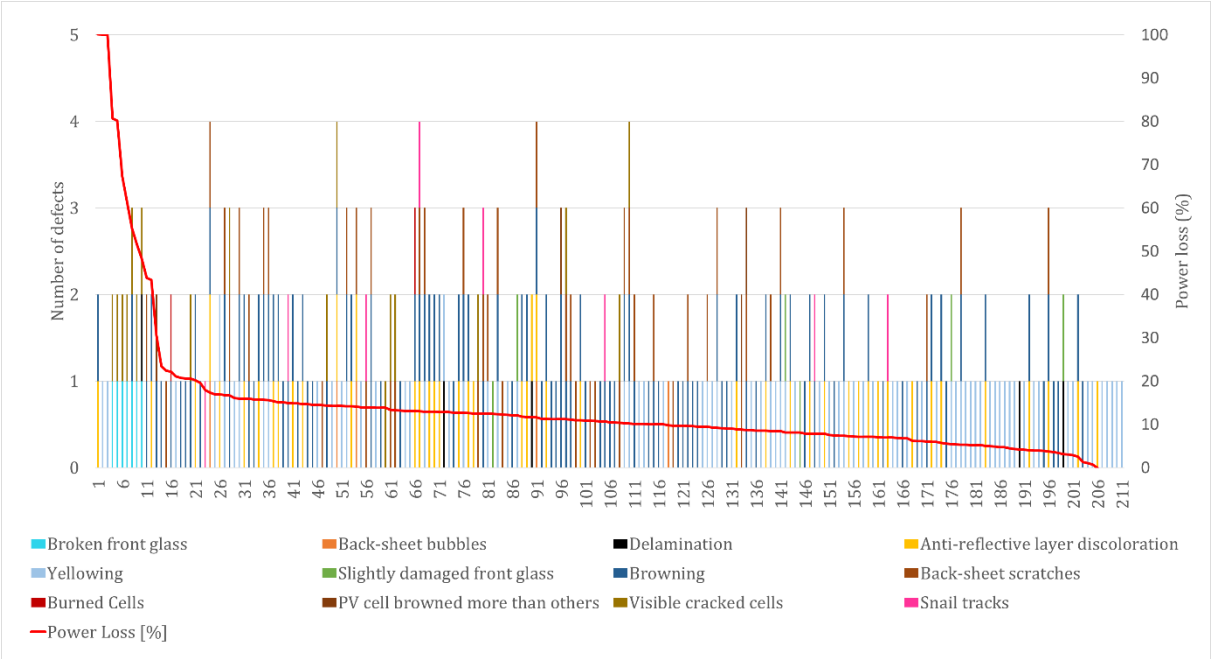

Fig. 5. Total number of visual defects in PV modules and its power loss associated

PV modules have been grouped according to the number of total defects found in each one. Fig. 6 shows the groups created and its power loss, where each point represents a single PV module. It can be seen that power loss can vary widely without having any correlation. However, there is a light growing trend in the case of PV modules affected by 4 defects.

PV modules with 100% of power loss were due to internal disconnection in the junction box or connectors internal failure, which were not visible during this test.

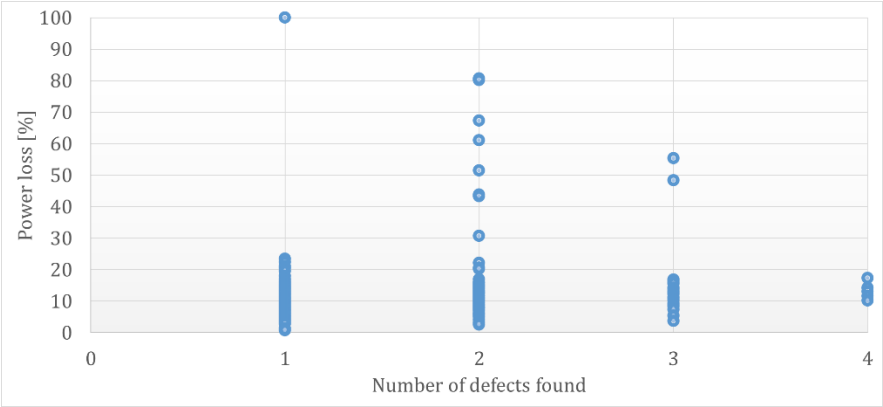

Fig. 6. Grouping of defectives PV modules and its power loss associated

345 *Table II: Analysis of visual defects*

Defects founds	Power loss range	Power loss over time Ref. [21]	Safety Ref. [21]	Occurrence	Interpretation of results	Final decision
Broken front glass	48.36 - 80.66%	Loss of mechanical integrity. The operation of the module would be impaired. Power loss below the detection limit.	Fire, electrical shock and physical danger.	1.94%	Great power loss and several safety problems	Non-acceptable
Back-sheet bubbles	9.77-17.33%	Power loss degradation saturates over time Degradation in steps over time	Electrical shock.	1.39%	Wide range of power loss	Acceptable
Delamination	3.13-48.36%	Power loss degradation saturates over time Degradation in steps over time	Electrical shock.	1.39%	Wide range of power loss	Acceptable
Anti-reflective layer discoloration	0 - 43,34%	Lower short-circuit current, likely caused by loss of transparency Linear-shaped power loss degradation over time Degradation in steps over time	This defect has no effect on safety.	12.78%	Wide range of power loss	Acceptable
Yellowing	0 - 21.08%	Lower short-circuit current, likely caused by loss of transparency Linear-shaped power loss degradation over time Degradation in steps over time	This defect has no effect on safety.	22.22%	Wide range of power loss	Acceptable
Slightly damaged front glass	3,13 – 12,43%	Linear-shaped power loss degradation over time Degradation in steps over time	This defect has no effect on safety.	1.67%	Wide range of power loss	Acceptable
Browning	1,13% - 55.31%	Linear-shaped power loss degradation over time	This defect has no effect on safety.	31.11%	Wide range of power loss	Acceptable
Back-sheet scratches	3.68 – 43,82%	-	It may affect the insulation properties.	13.06%	Wide range of power loss	Acceptable
Burn marks	13.06 – 22.15%	Power loss degradation saturates over time. Degradation in steps over time	Fire, electrical shock and physical danger.	0.56%	Considerable power loss and several safety problems.	Non-acceptable
PV cell browned more than others	8.74 – 30.65 %	Power loss degradation saturates over time	Fire.	1.11%	Wide range of power loss	Acceptable
Visible cracked cells	10.17 – 80.66%	Power loss degradation saturates over time Degradation in steps over time	Defect has no effect on safety.	5.00%	Wide range of power loss	Acceptable
Snail tracks	6.97 – 17.92%	Linear-shaped power loss degradation over time	Fire.	2,22%	Wide range of power loss	Acceptable

346

5.2. Electrical inspection: Power rating

Results obtained to all the sample modules have been grouped according to the manufacturer and presented in Fig. 7-9. In such figures, the measured peak power of each sample extrapolated to STC is shown. To be able to evaluate the results obtained, it has been added in these graphs the rated peak power in STC of each sample and several thresholds according to the degradation levels established in the acceptance/rejection criteria. Thresholds are defined as the value of peak power proportional to the limits established by the laboratory in the year 11 (<15% of R_T), the peak power when the sample will be considered as degraded (15-20% of R_T) and the peak power when the sample is considered as rejected (>20% of R_T).

Fig. 7 shows the peak power measured in STC of sample modules brand 1, where the 87.76% as resulted as fit, the 5.10% as degraded and the 7.14% as unfit.

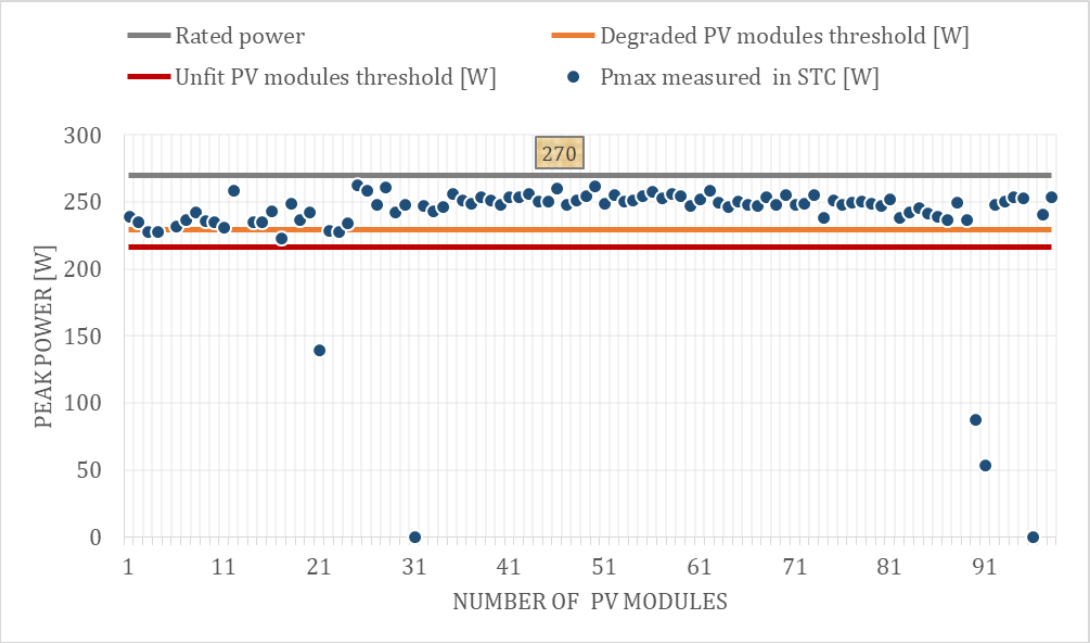

Fig. 7. Power rating results of PV modules brand 1

Fig. 8 shows the peak power measured in STC of sample modules brand 2 from 200Wp to 230Wp classes, where the 74.47% as resulted as fit, the 13.62% as degraded and the 11.91% as unfit.

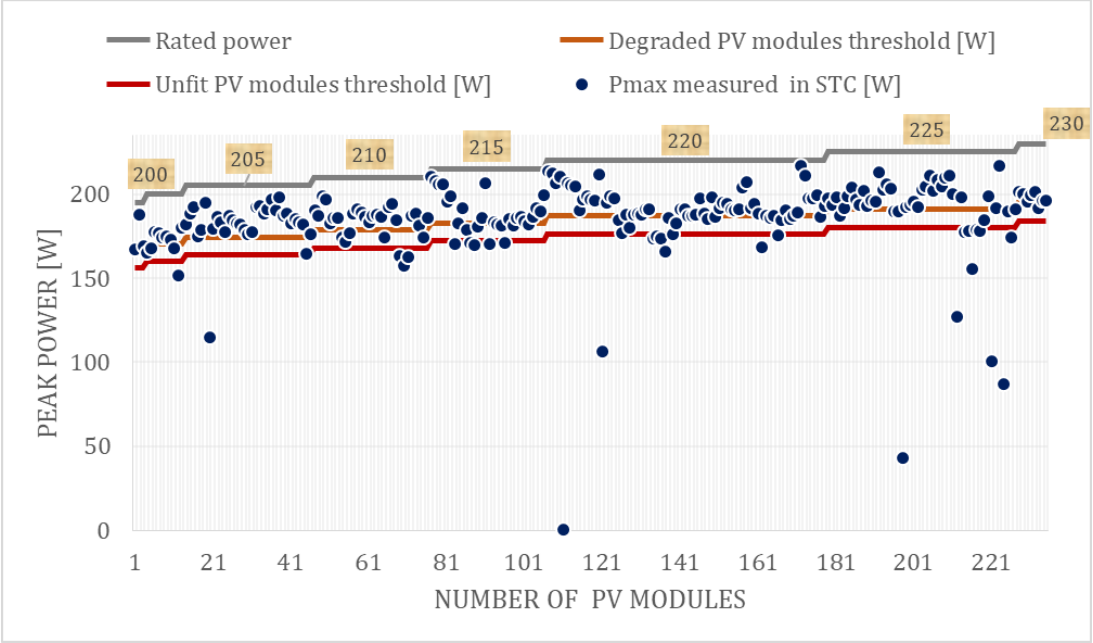

Fig. 8. Power rating results of PV modules brand 2

Fig. 9 shows the peak power measured in STC of PV modules sample modules brand 3 from 210Wp to 240Wp, where the 100% as resulted as fit. Based on the results obtained, this PV module brand has the best quality compared with the other brands installed in the PV plant. Due to the positive tolerance given by the manufacturer which is shown in Table I, in some cases, the peak power of the sample modules obtained got over the rated peak power obtained from the utility database.

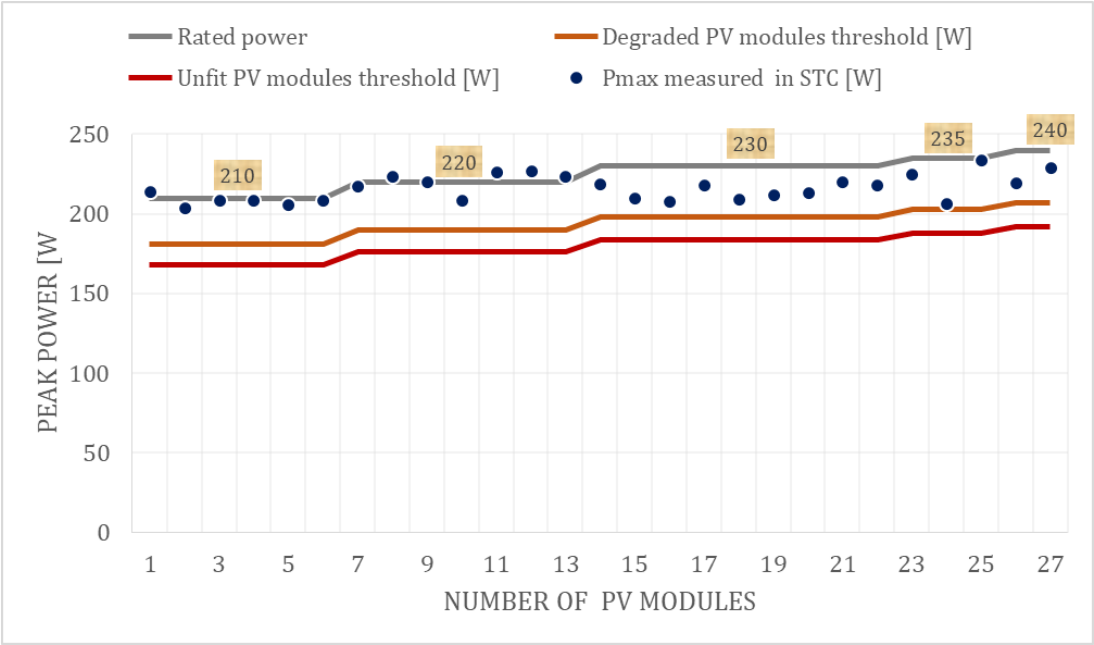

Fig. 9. Power rating results of PV modules brand 3.

5.3. Electroluminescence

All the sample modules have been analyzed according to the level of cracking presented in the acceptance/rejection criteria. Results are shown in Fig. 17. c). Additionally, other studies have been done to evaluate the relationship between PV cell cracks type C and power loss. These results are shown in fig. 10.

In this figure, it can be observed that there exits some kind of relationship between the PV cell cracks type C and the power loss. However, although the correlation between both parameters is better than what has been obtained in [40], it has been considered that it remains weak (R^2=0.5151). Others author in [21] considers that this relationship between the number of cell cracks in a PV module and its power loss is very noisy.

The red line drawn in Fig. 10 is the limit established by the laboratory for the evaluation of EL test. Thus, all sample modules that got over the red line had an area greater than the 8% affected by cracks type C and were all considers as non-acceptable. So, a total of 19 sample modules were rejected, of which 5 were modules brand 1 and 14 were modules brand 2.

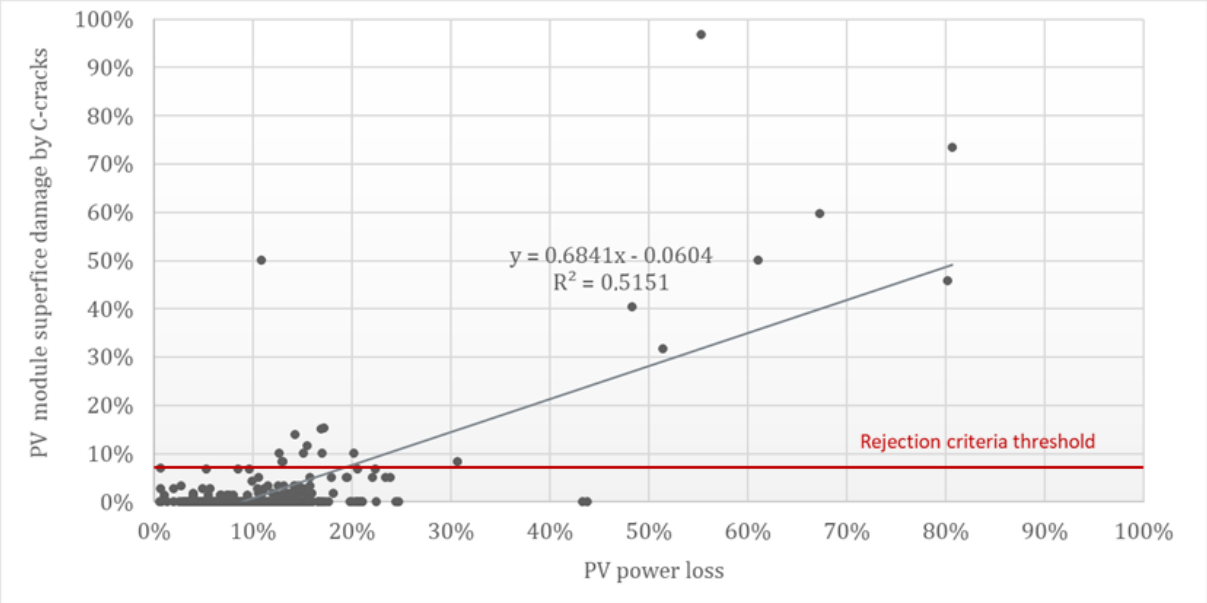

Fig. 10. Relationship between the PV module area damage by C-cracks and the power loss of the sample modules tested.

Prior to the laboratory tests, an IR inspection of the complete PV plant was carried out in order to evaluate the behaviour and thermal impacts under real operating conditions. The thermographic inspection was carried out from the rear of the modules in accordance with the IEC 62446-3 [30] standard and considering predefined criteria for the location and configuration of the

thermographic equipment [41]. Fig. 11 shows for each brand the percentage of PV modules with thermal incidents and the percentage of PV modules with hot spots or hot cells. In addition, the value of the maximum temperature measured in each case is indicated. In global terms, 0.79% of PV modules in the plant have some kind of thermal incidence, while 0.73% of PV modules have hot cells or hot spots.

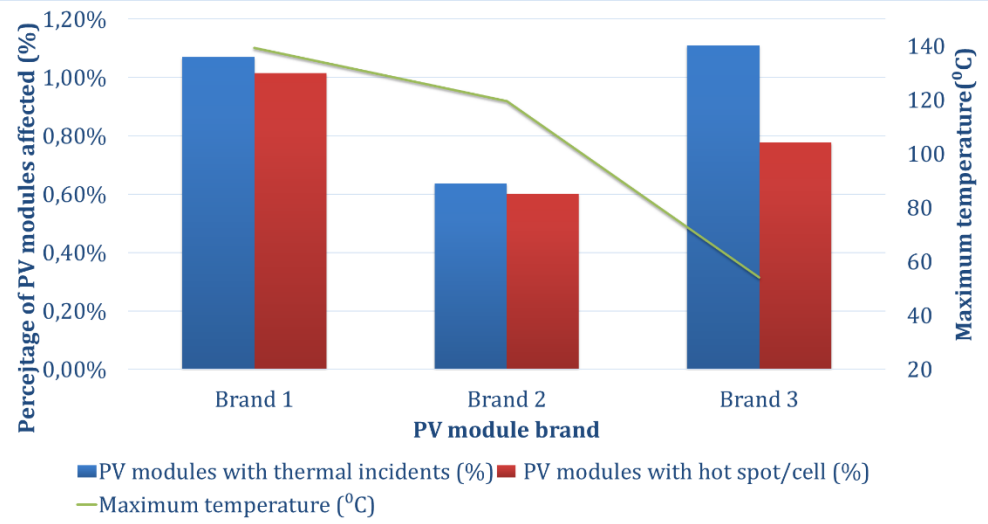

Fig. 11. Summary of IR inspection result according to PV module brand.

According to [12], cracks in cells, which temperature depends on the fracture characteristic and the ambient condition, may strongly impact the module performance. IR and EL test have not commonly shown similar results when both images are compared. Since both tests has been performed in different conditions, it may be caused because the contact resistance between the two sides of the micro-crack varies with module temperature and could be much larger during the day (when hot-spots are observed) than during the night or in a dark environment when EL images are obtained [40].

However, it has been observed that some results obtained from EL and IR images show a certain relationship between the inactive area and the hot-spot. Those modules affected by both cracks and hot cells have a greater impact on the module performance [42]. An example has been presented in this paper with the result obtained in the IR inspection made in-situ [28] and the EL test performed in the laboratory. The sample chosen was the PV module brand 1 of 270Wp, which showed a 49.49% of power loss during the I-V tracer test and some visible failures, such as broken front-glass and visual cracked cell, were found in the detailed visual inspection. Both defects are shown in fig. 12.

a) b)

Fig. 12. Visual Inspection a) Cracked cells b) Broken front glass

Fig. 13 shows both images, the IR image when the PV module was working under operating condition, and the EL image from the sample chosen. In this case, the EL test has been performed in a laboratory according to the methodology presented in this paper. The EL image shows several cracks in solar cells. The affected PV cell area of C-cracks was 40.28% of the PV module respectively, which meant that 59.72% of the area had non-significant power loss. The IR image, which was taken at the rear of the PV module, shows that a total of 7 PV cells were affected by thermal abnormalities.

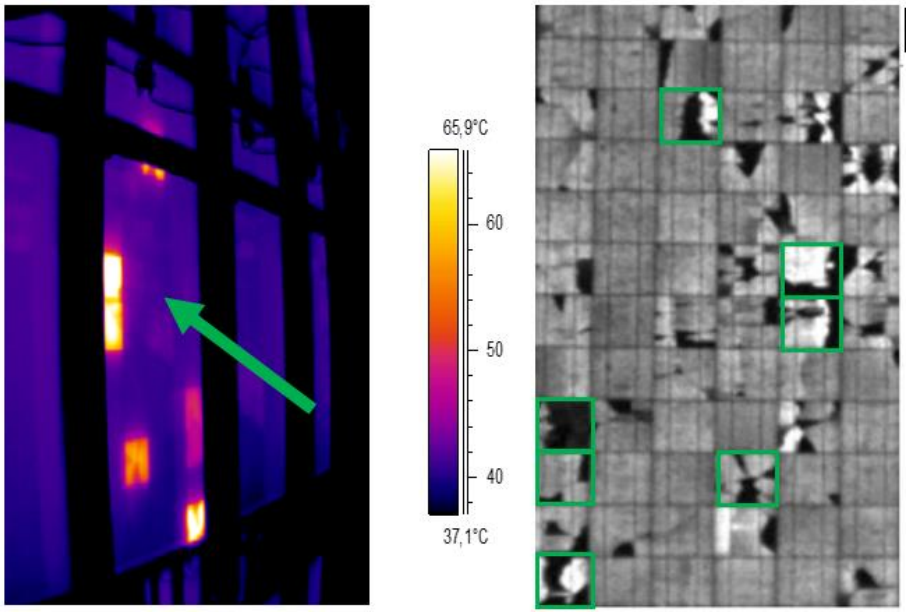

a) b)

Fig. 13 a) IR thermography (at the rear of the module), b) EL front-image at 100% of Isc

Both images were compared and it could be observed that all the thermal abnormalities found in the IR image were also reflected in the EL image, which have been highlighted in a green box. According to [43], this correlation occurs when the temperature of the cell increases 10-20°C, having the unproductive cracked area a similar behaviour of a shaded area.

5.4. Electrical insulation

Fig. 14-16 show the results of the electrical insulation test for sample modules brand 1, brand 2 and brand 3 respectively. The orange line drawn in such figures is the rejected criteria reference value established by the IEC 61215-2:2016 [33].

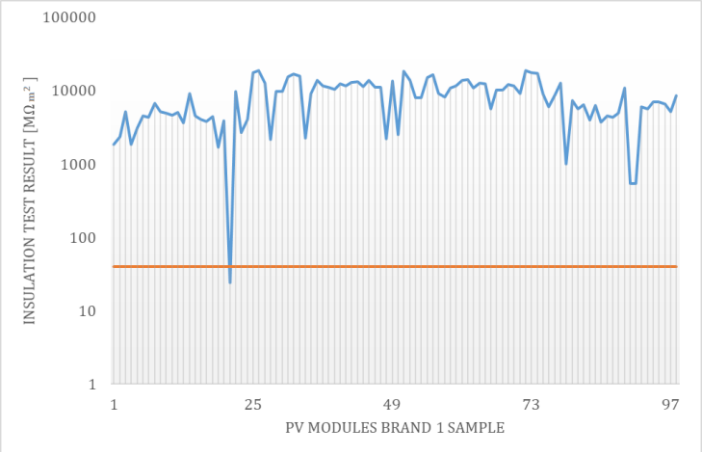

Fig. 14. Electrical insulation results in sample module brands 1.

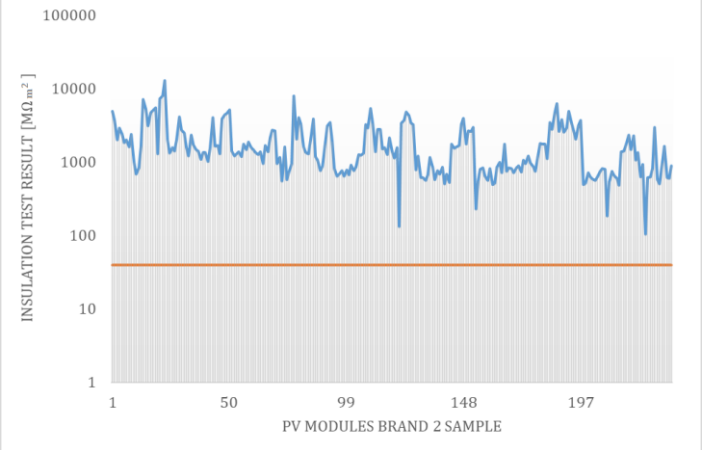

Fig. 15. Electrical insulation results in PV module sample module brands 2.

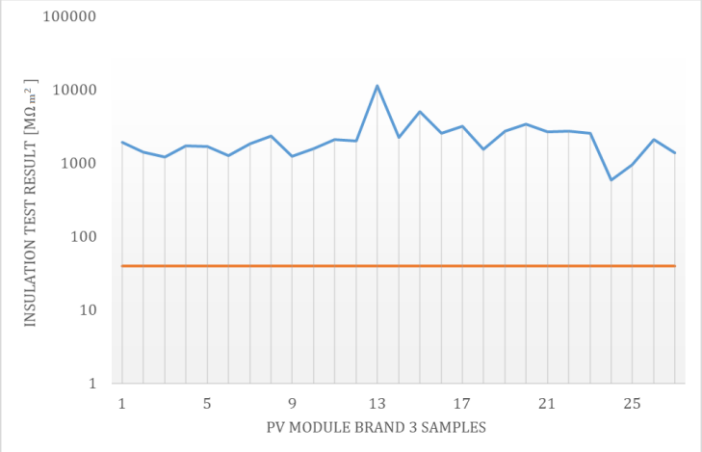

Fig. 16. Electrical insulation results in PV module sample module brands 3.

From all the sample modules tested and as it is shown in fig. 14, only one module has resulted as non-acceptable. The PV module insulation resistance measured in such rejected sample was 24.06 $M\Omega \cdot m^2$.

5.5. Overall result following the acceptance/rejection criteria established

The overall results of the 4 test performed following the evaluation of each one and the acceptance/rejection criteria established in section 4 are shown in Fig. 17. Results for each test are shown by PV module class.

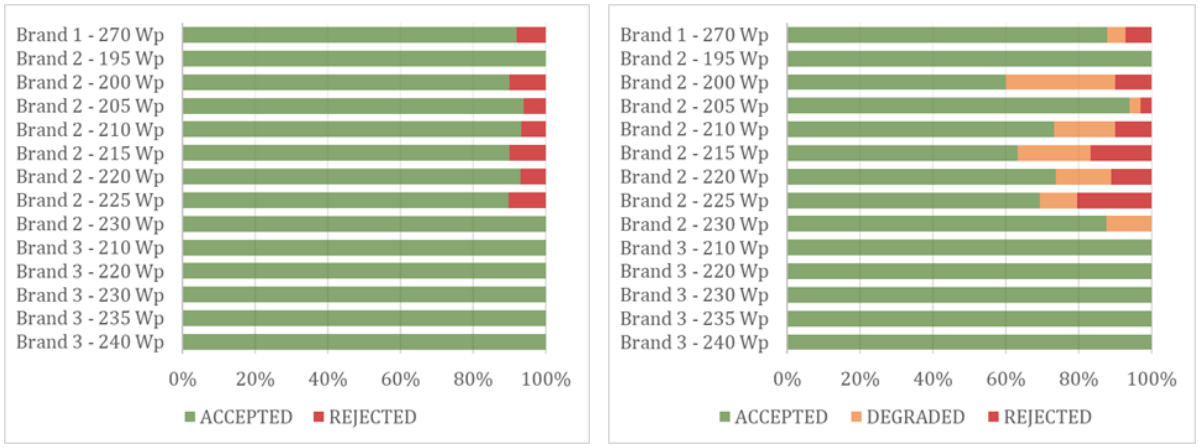

a) Detailed visual inspection results b) Power rating results

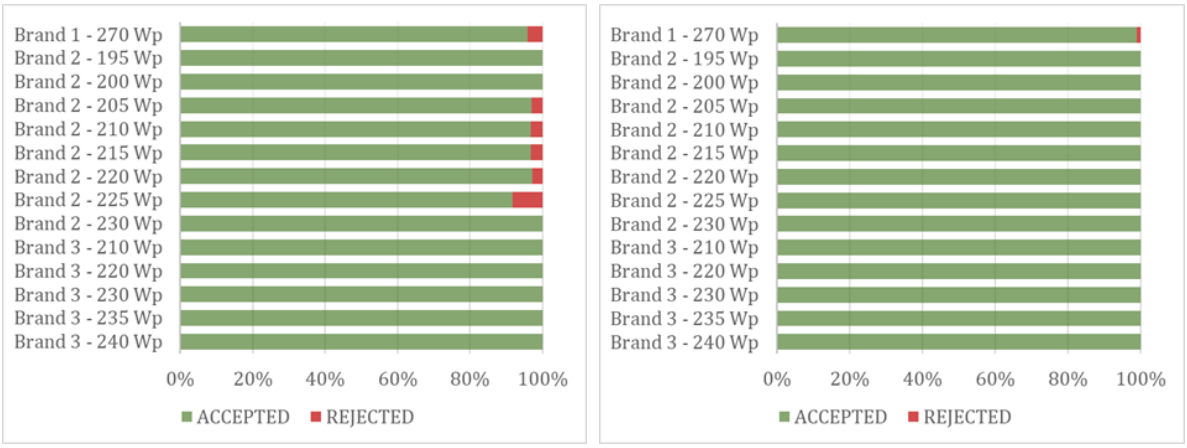

c) Electroluminescence results d) Electrical insulation results

Fig. 17. Overall result by each test performed

Fig. 17. a) shows the results of the detailed visual inspection where the accepted ones have been colored in green while rejected ones have been colored in red. The PV module class with the greatest percentage of failure has been the brand 2 of 225Wp with the 8.16% followed by brand 2 of 215Wp and 210Wp, both with the 3.33%. Clustering by manufacturer, the percentage of failures found in brand 1, brand 2 and brand 3 would be the 4.08%, 3.83% and 0.00% respectively. Globally, only the 3.61% were rejected in the detailed visual inspection.

Fig. 17 b) shows the results of the power rating test and the acceptance/rejection criteria, where accepted, degraded and rejected sample modules were colored in green, orange and red respectively. In this case, the PV module brand 2 of 225Wp, 215Wp and 220Wp, with the 20.41%, 16.67% and 11.11% respectively, were the classes with the greatest percentage of non-acceptance. In terms of degradation, the PV module brand 2 of 200Wp, 215Wp and 210Wp, with the 30.00%, 20.00% and 16.67% respectively, were the most affected by. Clustering by manufacturer, the percentage of rejected of brand 1, brand 2 and brand 3 were 7.14%, 11.91% and 0.00% respectively. If all the sample modules are grouped, the 80.00% of the PV modules tested were found to be in good condition, the 10.27% degraded and the 9.72% rejected.

Fig. 17 c) shows the results of electroluminescence test clustered by PV module class, where the percentage of accepted and rejected PV modules classes are colored in green and red respectively. The PV module class with the greatest percentage of non-acceptance has been the brand 2 of 225Wp, with the 10.20%, followed by the PV module brand 2 of 215Wp and 200Wp, both with the 10%. Clustering by manufacturer, the percentage of rejected PV modules in brand 1, brand 2 and brand 3 was 8.16%, 7.66% and 0.00% respectively. As a global result, the 7.22% of the sample modules were rejected.

And finally, Fig. 17 d) shows the results of the electrical insulation test, where only one sample was rejected which corresponded to the brand 1 of 270Wp.

6. Annual degradation rates

Once all the sample modules were evaluated according with the acceptance/rejection criteria established, the ADR_{Pmax}, which eq. is showed in (3), was obtained for each one. The ADR_{Pmax} (3) of each sample were clustered by the manufacturer to evaluate and compare the degradation between them. Then, the histogram and its corresponding probability density function (PDF) has been obtained. All the PDFs obtained resulted in fitting well with a normal distribution. These PDFs have been obtained applying a non-linear regression fitting the least square using the Gauss-Newton algorithm.

Fig. 18, 19 and 20 show the histogram and its corresponding PDF of PV module brand 1, 2 and 3 respectively, which are all compared in Fig.22. Table III shows, the annual average degradation rate for each manufacturer and the lower and upper bounds with a confidence interval (c.i.) of 95% according to a normal distribution.

Table III: annual degradation rate for each manufacturer PV-module

	lower c.i.	mean	upper c.i.	
PV module sample brand 1	0.624992	0.6813	0.737608	%/year
PV module sample brand 2	1.063434	1.1134	1.163366	%/year
PV module sample brand 3	0.110553	0.2792	0.447847	%/year

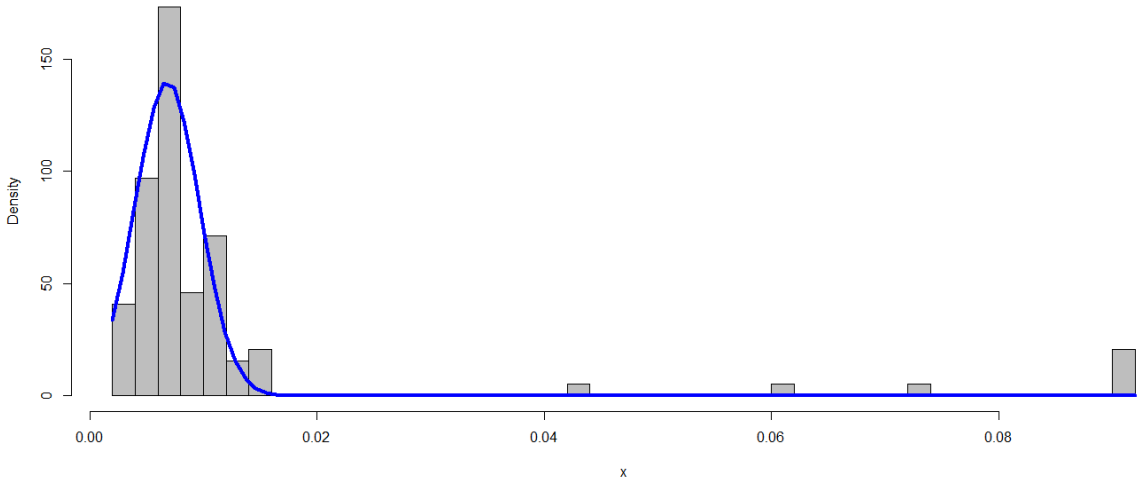

Fig. 18. Histogram and approximation of PDF (normal distribution, $\bar{x} = 0.00683, sd\ 0.002844$) of the PV module sample brand 1.

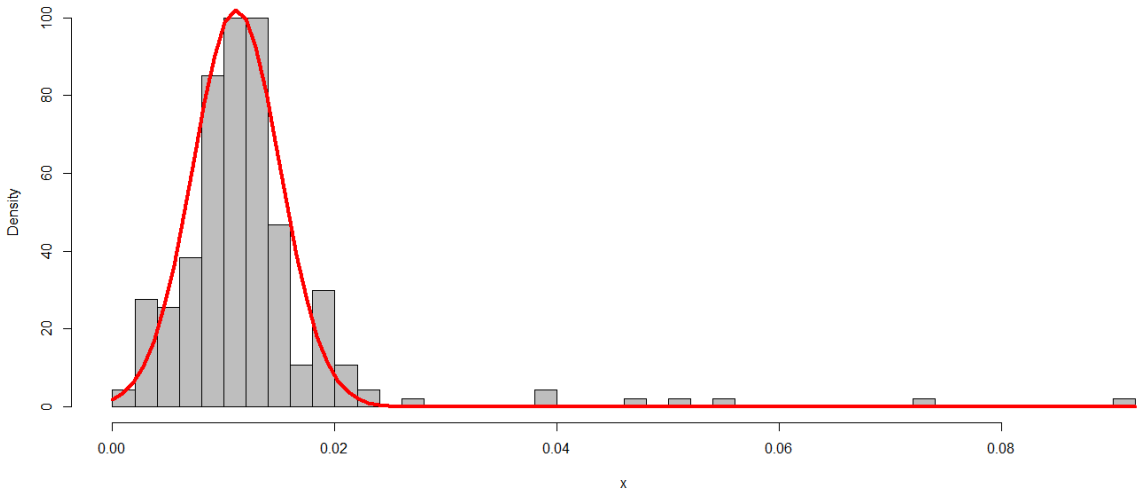

Fig. 19. Histogram and approximation of PDF (normal distribution, $\bar{x} = 0.011134, sd = 0.003908$) of the PV module sample brand 2.

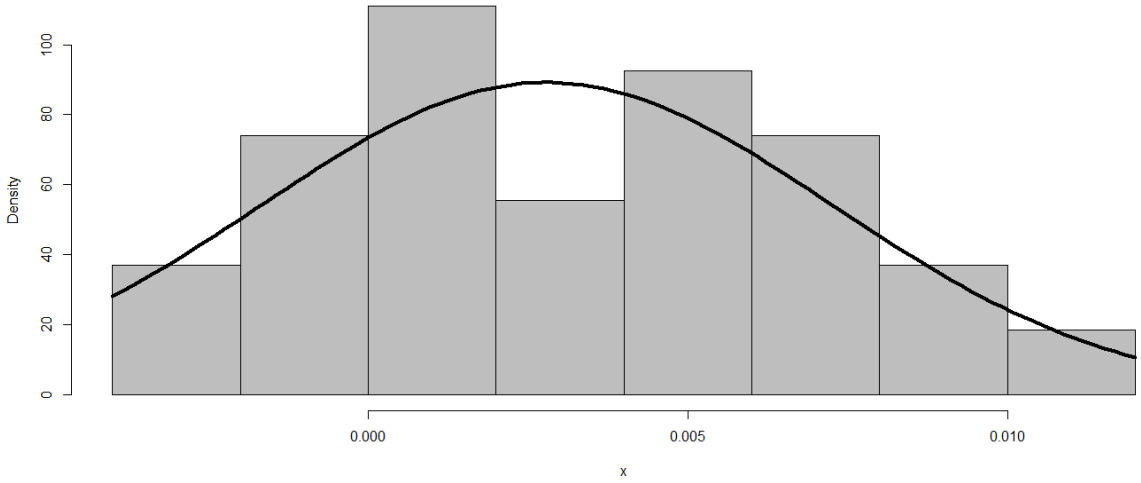

Fig. 20. Histogram and approximation of PDF (normal distribution, $\bar{x} = 0.002792, sd = 0.004471$) of the PV module sample brand 3.

Although all the sample modules presented in this study came from the same areas which shared the same climatic conditions, a different average annual degradation was obtained in each one. Fig. 21 shows the comparison of the resulted PDF for each manufacturer, where it can be seen that the greater annual degradation comes from PV sample brand 2. By contrast, the PV module that showed the lower annual degradation was brand 3. If both average results are compared, there is a difference between them of 0.83%/year, which highlight the importance of using one brand or other.

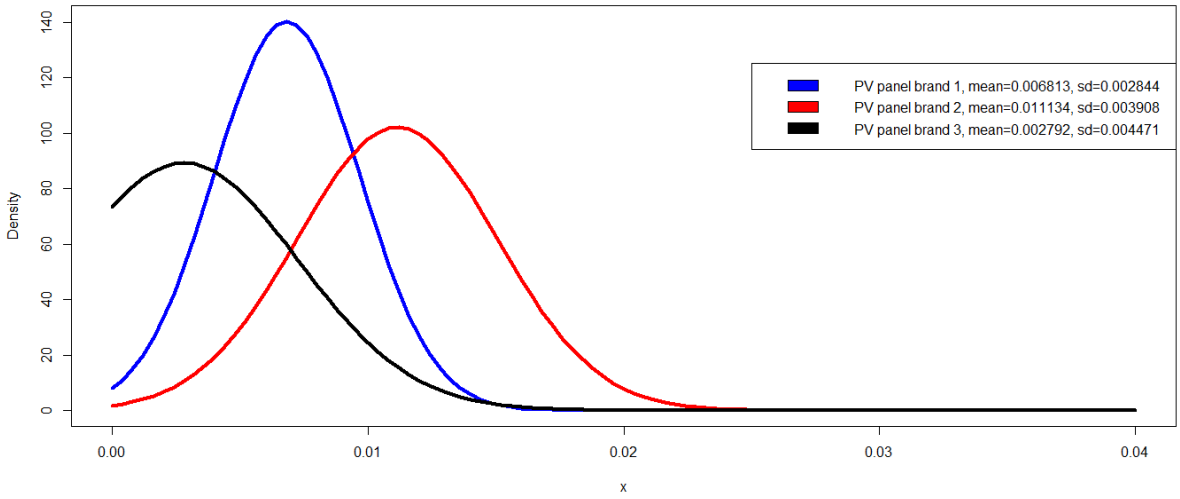

Fig. 21. Comparison of PV-module brand 1, 2 and 3 PDFs

Fig. 22 shows the histogram and its corresponding PDF when all the sample modules are studied together. In this case, the PDF obtained also resulted in fitting well with a normal distribution, which has been obtained applying a non-linear regression fitting the least square using the Gauss-Newton algorithm. The average annual degradation rate resulted in 0.94%/year while its lower and upper bounds with a c.i. of 95% according to a normal distribution were 0.89%/year and 0.99%/year respectively.

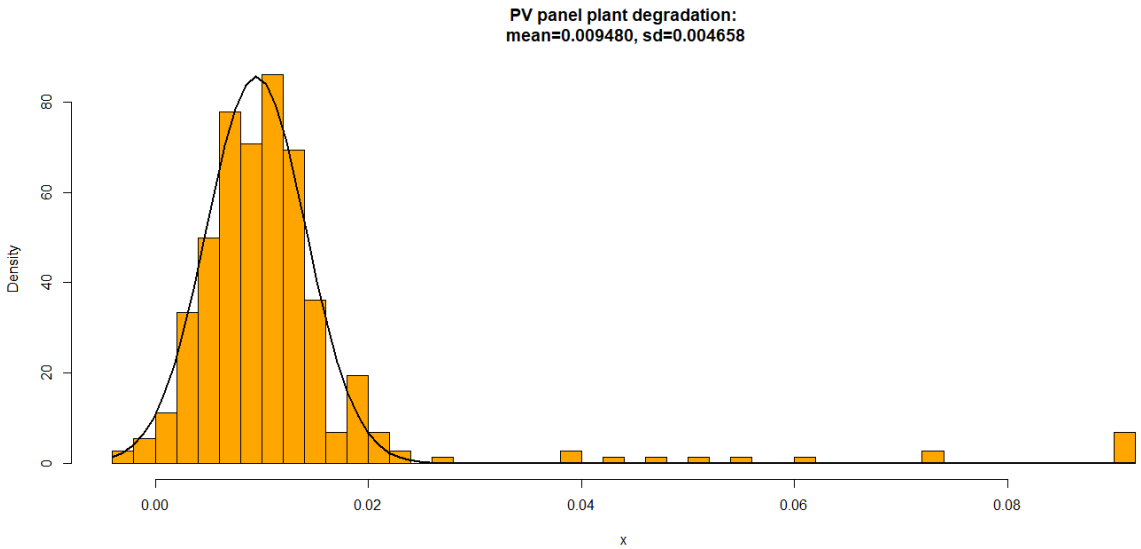

Fig. 22. Histogram and approximation of PDF (normal distribution, $\bar{x} = 0.009480, sd = 0.004658$) to all the sample modules.

The variation of P_{max} losses with losses in Isc, Voc and fill factor (FF) has been also studied, where Isc and FF losses were dominant while V_{oc} had weakness correlation. According to [7], the impact

of the Isc on the power loss may be caused by the influence of some observable defects that lead to reduce the light transmission to the solar cells.

7. Conclusion

- The probability method selected was a stratified random sampling with proportional allocation. A total of 360 PV modules were subjected to the following tests: detailed visual inspection, power rating, electroluminescence, and electrical insulation.
- An annual degradation of 0.681%, 1.113% and 0.279% were obtained to brand 1, 2 and 3 respectively. Which meant that despite being all of them working under the same conditions of location, operation and maintenance, some PV module brands showed worst levels of degradation after its years of operation.
- When all brands were grouped together, a global average annual degradation of 0.9480% was obtained, being the losses in the short-circuit current and fill factor the dominant factors.
- The browning, yellowing, back sheet scratches and anti-reflective layer were the most observed defect over the sample modules.
- In global terms, the 0.79% of PV modules in the PV plant had some kind of thermal incidence and the 0.73% of PV modules had hot cells or hot spots.
- According to the power rating test, which authors considered as the most suitable as a global result, and its acceptance/rejection criteria established in the methodology, the 80.01% of the PV modules tested were found to be in good condition, the 10.27% degraded and the 9.72% rejected.

This evaluation could be applied to other photovoltaic plants with different conditions to analyze its performance.

References

[1] Solar Power Europe, "Global Market Outlook For Solar Power: 2020 - 2024," 2020. doi: 10.4018/978-1-7998-4607-9.ch006.

[2] I. International Renewable Energy Agency, "Future of solar photovoltaic. Deployment, investment, technology, grid integration and socio-economic aspects," *(A Global Energy Transformation: paper), International Renewable Energy Agency (IRENA), Abu Dhabi.* p. 88, 2019, [Online]. Available: www.irena.org/publications.

[3] L. Peters and R. Madlener, "Economic evaluation of maintenance strategies for ground-mounted solar photovoltaic plants," *Appl. Energy*, vol. 199, pp. 264–280, 2017, doi: 10.1016/j.apenergy.2017.04.060.

[4] Solar Power Europe, *Operation & Maintenance Best Practice Guidelines / Version 4.0*. 2019.

[5] M. Kumar and A. Kumar, "Performance assessment and degradation analysis of solar photovoltaic technologies: A review," *Renew. Sustain. Energy Rev.*, vol. 78, no. November

2016, pp. 554–587, 2017, doi: 10.1016/j.rser.2017.04.083.

[6] D. C. Jordan and S. R. Kurtz, “Photovoltaic degradation rates - An Analytical Review,” *Prog. Photovoltaics Res. Appl.*, vol. 21, no. 1, pp. 12–29, 2013, doi: 10.1002/pip.1182.

[7] D. A. Quansah and M. S. Adaramola, “Ageing and degradation in solar photovoltaic modules installed in northern Ghana,” *Sol. Energy*, vol. 173, no. August, pp. 834–847, 2018, doi: 10.1016/j.solener.2018.08.021.

[8] M. A. Islam, M. Hasanuzzaman, and N. A. Rahim, “A comparative investigation on in-situ and laboratory standard test of the potential induced degradation of crystalline silicon photovoltaic modules,” *Renew. Energy*, vol. 127, pp. 102–113, 2018, doi: 10.1016/j.renene.2018.04.051.

[9] T. Ishii and A. Masuda, “Annual degradation rates of recent crystalline silicon photovoltaic modules.,” *Prog. Photovoltaics Res. Appl.*, no. 25, pp. 953–967, 2017, doi: 10.1002/pip.2903.

[10] C. Schuss, K. Leppanen, J. Saarela, T. Fabritius, B. Eichberger, and T. Rahkonen, “Detecting defects in photovoltaic modules with the help of experimental verification and synchronized thermography,” *Conf. Rec. - IEEE Instrum. Meas. Technol. Conf.*, vol. 2015-July, pp. 97–102, 2015, doi: 10.1109/I2MTC.2015.7151247.

[11] J. A. Tsanakas, L. Ha, and C. Buerhop, “Faults and infrared thermographic diagnosis in operating c-Si photovoltaic modules: A review of research and future challenges,” *Renew. Sustain. Energy Rev.*, vol. 62, pp. 695–709, 2016, doi: 10.1016/j.rser.2016.04.079.

[12] C. Buerhop, D. Schlegel, M. Niess, C. Vodermayer, R. Weißmann, and C. J. Brabec, “Reliability of IR-imaging of PV-plants under operating conditions,” *Sol. Energy Mater. Sol. Cells*, vol. 107, pp. 154–164, 2012, doi: 10.1016/j.solmat.2012.07.011.

[13] S. Blanc, P. Yuste, A. Lorente, and J. J. Serrano, “An integral and flexible wireless power monitoring system,” *Renew. Energy Power Qual. J.*, vol. 1, no. 9, pp. 1290–1293, 2011, doi: 10.24084/repqj09.625.

[14] D. Thevenard, L. Dignard-Bailey, S. Martel, and D. Turcotte, “Performance monitoring of a northern 3.2 KWp grid-connected photovoltaic system,” *Conf. Rec. IEEE Photovolt. Spec. Conf.*, vol. 2000-Janua, pp. 1711–1714, 2000, doi: 10.1109/PVSC.2000.916233.

[15] B. Ando, S. Baglio, A. Pistorio, G. M. Tina, and C. Ventura, “Sentinella: Smart Monitoring of Photovoltaic Systems at Panel Level,” *IEEE Trans. Instrum. Meas.*, vol. 64, no. 8, pp. 2188–2199, 2015, doi: 10.1109/TIM.2014.2386931.

[16] A. Livera, M. Theristis, G. Makrides, and G. E. Georghiou, “Recent advances in failure diagnosis techniques based on performance data analysis for grid-connected photovoltaic systems,” *Renew. Energy*, vol. 133, pp. 126–143, 2019, doi: 10.1016/j.renene.2018.09.101.

[17] A. Sayyah, M. N. Horenstein, and M. K. Mazumder, “Energy yield loss caused by dust

596 deposition on photovoltaic panels," *Sol. Energy*, vol. 107, pp. 576–604, 2014, doi:
597 10.1016/j.solener.2014.05.030.

598 [18] P. Sánchez-Friera, M. Piliougine, J. Peláez, J. Carretero, and M. S. De Cardona, "Analysis of
599 degradation mechanisms of crystalline silicon PV modules after 12 years of operation in
600 Southern Europe," *Prog. Photovoltaics Res. Appl.*, vol. 19, no. 6, pp. 658–666, Sep. 2011,
601 doi: 10.1002/pip.1083.

602 [19] A. Carullo and A. Vallan, "Outdoor experimental laboratory for long-term estimation of
603 photovoltaic-plant performance," *IEEE Trans. Instrum. Meas.*, vol. 61, no. 5, pp. 1307–
604 1314, May 2012, doi: 10.1109/TIM.2011.2180972.

605 [20] M. A. Munoz, M. C. Alonso-García, N. Vela, and F. Chenlo, "Early degradation of silicon PV
606 modules and guaranty conditions," *Sol. Energy*, vol. 85, no. 9, pp. 2264–2274, 2011, doi:
607 10.1016/j.solener.2011.06.011.

608 [21] IEA-PVPS Task 13, "Review of Failures of Photovoltaic Modules," 2014. doi: 978-3-
609 906042-16-9.

610 [22] Y. Hu, W. Cao, J. Ma, S. J. Finney, and D. Li, "Identifying PV module mismatch faults by a
611 thermography-based temperature distribution analysis," *IEEE Trans. Device Mater.*
612 *Reliab.*, vol. 14, no. 4, pp. 951–960, 2014, doi: 10.1109/TDMR.2014.2348195.

613 [23] S. A. Rahaman, T. Urmee, and D. A. Parlevliet, "PV system defects identification using
614 Remotely Piloted Aircraft (RPA) based infrared (IR) imaging: A review," *Sol. Energy*, vol.
615 206, no. April, pp. 579–595, 2020, doi: 10.1016/j.solener.2020.06.014.

616 [24] E. Caamaño, E. Lorenzo, and R. Zilles, "Quality control of wide collections of PV modules:
617 lessons learned from the IES experience," *Prog. Photovoltaics Res. Appl.*, vol. 7, no. 2, pp.
618 137–149, 1999, doi: 10.1002/(sici)1099-159x(199903/04)7:2<137::aid-
619 pip249>3.3.co;2-3.

620 [25] E. S. Kopp, V. P. Lonij, A. E. Brooks, P. L. Hidalgo-Gonzalez, and A. D. Cronin, "I-V curves
621 and visual inspection of 250 PV modules deployed over 2 years in tucson," *Conf. Rec. IEEE*
622 *Photovolt. Spec. Conf.*, pp. 3166–3171, 2012, doi: 10.1109/PVSC.2012.6318251.

623 [26] J. E. F. da Fonseca, F. S. de Oliveira, C. W. Massen Prieb, and A. Krenzinger, "Degradation
624 analysis of a photovoltaic generator after operating for 15 years in southern Brazil," *Sol.*
625 *Energy*, vol. 196, no. November 2019, pp. 196–206, 2020, doi:
626 10.1016/j.solener.2019.11.086.

627 [27] D. D. P. and V. L. Alessandro Massi Pavan, Adel Mellit, "A study on the mismatch effect due
628 to the use of different photovoltaic modules classes in large-scale solar parks," *Prog.*
629 *Photovoltaics Res. Appl.*, vol. 22, pp. 332–345, 2014, doi: 10.1002/pip.

630 [28] J. A. Clavijo-Blanco, G. Álvarez-Tey, N. Saborido-Barba, J. L. Barberá-González, C. García-
631 López, and R. Jiménez-Castañeda, "Quality inspection of a 2.85 MW PV power plant under
632 mismatch loss due to different classes of pv module installed," *Renew. Energy Power Qual.*

633 *J.*, vol. 18, no. 18, pp. 276–281, 2020, doi: 10.24084/repqj18.298.

634 [29] International Electrotechnical Commission, *IEC 61215-1-1:2016. Terrestrial photovoltaic*
635 *(PV) modules. Design qualification and type approval. Part 1-1: Special requirements for*
636 *testing of crystalline silicon photovoltaic (PV) modules.* 2016.

637 [30] International Electrotechnical Commission, *IEC TS 62446-3. PV Systems-Requirements for*
638 *testing, documentation and maintenance. Part 3: Photovoltaic modules and plants- Outdoor*
639 *infrared thermography.*, vol. 7, no. 4. 2015.

640 [31] International Electrotechnical Commission, *IEC 61724-1:2017. Photovoltaic system*
641 *performance - Part 1: Monitoring*. 2018.

642 [32] International Organization for Standardization, "ISO 2859-1:1999 Sampling procedures
643 for inspection by attributes. Part 1: Sampling schemes indexed by acceptance quality limit
644 (AQL) for lot-by-lot inspection," *Iso*, vol. 2nd editio. p. 94, 1999, doi: 10.5594/J03363.

645 [33] International Electrotechnical Commission, *IEC-61215-2. Terrestrial photovoltaic (PV)*
646 *modules. Design qualification and type an approval. Part 2: Test procedures.* 2016.

647 [34] International Electrotechnical Commission, *IEC 60891:2009. Photovoltaic devices -*
648 *Procedures for temperature and irradiance corrections to measured I-V characteristics.*
649 2009.

650 [35] International Electrotechnical Commission, *IEC TS 60904-13 Photovoltaic devices-Part 13:*
651 *Electroluminescence of photovoltaic modules*. 2018.

652 [36] W. Muehleisen *et al.*, "Outdoor detection and visualization of hailstorm damages of
653 photovoltaic plants," *Renew. Energy*, vol. 118, pp. 138–145, 2018, doi:
654 10.1016/j.renene.2017.11.010.

655 [37] M. S. Chowdhury *et al.*, "An overview of solar photovoltaic panels' end-of-life material
656 recycling," *Energy Strategy Reviews*. 2020, doi: 10.1016/j.esr.2019.100431.

657 [38] C. R. Osterwald, J. Adelstein, J. A. Del Cueto, B. Kroposki, D. Trudell, and T. Moriarty,
658 "Comparison of degradation rates of individual modules held at maximum power," *Conf.*
659 *Rec. 2006 IEEE 4th World Conf. Photovolt. Energy Conversion, WCPEC-4*, vol. 2, pp. 2085–
660 2088, 2006, doi: 10.1109/WCPEC.2006.279914.

661 [39] I. Kunze, S. Kajari-schr, X. Breitenmoser, and B. Bjørneklett, "The risk of power loss in
662 crystalline silicon based photovoltaic modules due to micro-cracks," *Sol. Energy Mater.*
663 *Sol. Cells*, vol. 95, pp. 1131–1137, 2011, doi: 10.1016/j.solmat.2010.10.034.

664 [40] R. Moretón, E. Lorenzo, and L. Narvarte, "Experimental observations on hot-spots and
665 derived acceptance/rejection criteria," *Sol. Energy*, vol. 118, pp. 28–40, 2015, doi:
666 10.1016/j.solener.2015.05.009.

667 [41] G. Álvarez-Tey, R. Jiménez-Castañeda, and J. Carpio, "Analysis of the configuration and the

location of thermographic equipment for the inspection in photovoltaic systems," *Infrared Phys. Technol.*, vol. 87, pp. 40–46, 2017, doi: 10.1016/j.infrared.2017.09.022.

[42] S. Chattopadhyay *et al.*, "Correlating infrared thermography with electrical degradation of PV modules inspected in all-india survey of photovoltaic module reliability 2016," *IEEE J. Photovoltaics*, vol. 8, no. 6, pp. 1800–1808, 2018, doi: 10.1109/JPHOTOV.2018.2859780.

[43] M. Garcia, L. Marroyo, E. Lorenzo, J. Marcos, and M. Pérez, "Observed degradation in photovoltaic plants affected by hot-spots," *Prog. Photovoltaics Res. Appl.*, vol. 22, pp. 1292–1301, 2013, doi: 10.1002/pip.